Journal of Reproduction and Development, Vol. 66, No 6, 2020

—Original Article—

CircPlekha7 plays an anti-fibrotic role in intrauterine adhesions by modulating endometrial stromal cell proliferation and apoptosis

Wei XIE[1)*], Min HE[2)*], Yuhuan LIU[1)], Xiaowu HUANG[1)], Dongmei SONG[1)] and Yu XIAO[1)]

[1)]*Hysteroscopic Centre, Fu Xing Hospital, Capital Medical University, Beijing100038, China*
[2)]*Department of Reproductive Medicine, The Second Affiliated Hospital of Zhengzhou University, Zhengzhou 450014, China*

Abstract. Circular RNA (circRNA) plays a key role in the development and progression of several diseases; however, its role in intrauterine adhesions (IUAs) is not well understood. This study aims to investigate the expression profiles and potential role of circRNA in IUA. RNA-sequencing was performed to screen for abnormally expressed circRNAs in TGF-β1-induced IUA endometrial stromal cell (ESC) model (IUA group) and an SMAD3 inhibitor, SIS3-treated IUA ESC model (SIS3 group). Gene Ontology enrichment and Kyoto Encyclopedia of Genes and Genomes pathway analyses were performed to uncover the key functions and pathways. Interaction networks were constructed and analyzed based on the competing endogenous RNA hypothesis of circRNA. CircRNAs were validated by Sanger sequencing and quantitative polymerase chain reaction (qPCR). Cell proliferation and apoptosis were measured using MTS and flow cytometry, respectively. The protein and mRNA expression levels of fibrosis-related proteins were measured using western blotting and reverse transcription–qPCR, respectively. A total of 66 circRNAs were differentially expressed between the IUA and SIS3 groups. CircPlekha7 was identified as one of the significantly upregulated circRNAs in the SIS3 group. Overexpression of circPlekha7 enhanced apoptosis, decreased the viability of ESCs, and suppressed the expression of *α-SMA*, *collagen I*, and *SMAD3* in ESCs; whereas knockdown of circPlekha7 exhibited opposite results. Altogether, the results indicate that circPlekha7 plays an anti-fibrotic role in IUA and may serve as a promising prognostic biomarker for patients with IUA. Therefore, overexpression of circPlekha7 could be a potential treatment strategy for IUA.

Key words: circPlekha7, Competing endogenous RNA, Intrauterine adhesions, RNA-sequencing

(**J. Reprod. Dev. 66:** 493–504, 2020)

Intrauterine adhesions (IUAs, also referred to as Asherman's syndrome or intrauterine synechiae) are bands of fibrous tissue that form in the endometrial cavity, often in response to a uterine procedure. IUAs contribute to infertility and/or recurrent pregnancy loss in women [1]. The characteristic symptoms of IUAs include menstrual disturbance, cyclical pelvic pain, recurrent abortions, and infertility [2, 3]. The principal cause of IUAs is endometrial trauma caused by surgical procedures, including curettage, cesarean section, and hysteromyomectomy, which may injure the endometrial basal layer. Tuberculosis and other infections may also result in chronic inflammation of the endometrium (endometritis). Trauma to and/or infection of the uterine lining may lead to formation of IUAs or destruction of the endometrial lining, resulting in the loss of spontaneous endometrium recovery and angiogenesis [4]. IUAs are characterized by the buildup of scar tissues between the inner walls of the uterus causing the walls to bind together. Endometrial fibrosis is the main pathological feature of IUA. In IUA, the endometrial stroma is mainly replaced by excessive fibrous tissues that are avascular and unresponsive to hormonal stimulation [5]. Transforming growth factor β (TGF-β) is one of the most potent inducers of fibrogenesis [6]. It plays a central role in modulating fibroblast phenotype and function during wound healing and tissue repair, and it is strongly linked to the deposition and remodeling of the extracellular matrix (ECM) [7]. TGF-β activation is associated with excessive scarring and fibrosis [8], and blockade of TGF-β activity reduces scarring [9]. TGF-β has been shown to induce a reversible epithelial to mesenchymal transdifferentiation in epithelial cells [10]. TGF-β signaling is involved in the differentiation of fibroblasts into myofibroblasts, which primarily produce large amounts of ECM proteins [11]. In addition, TGF-β is known to induce the expression of ECM proteins and *α-SMA* by activating the downstream mediators SMAD2 and SMAD3, and is implicated in the progression of multiple fibrotic diseases [12]. SIS3, a potent and selective inhibitor of SMAD3, inhibits the signaling of activin as well as TGF-β1 [13, 14].

Circular RNAs (circRNAs) are a novel subclass of endogenous noncoding RNAs, characterized by a covalently closed loop structure without a 5' cap and a 3' poly A tail [15, 16]. In recent years, circRNAs have attracted the attention of researchers worldwide because they play an indispensable role in the occurrence and development of many diseases by acting as miRNA sponges, protein binding molecules, and transcriptional regulators [17]. Emerging pieces of evidence have confirmed that circRNAs participate in the regulation of various biological processes, including cell proliferation, cell transition,

Received: December 31, 2019
Accepted: July 14, 2020
Advanced Epub: August 15, 2020

Correspondence: Y Xiao (e-mail: rain.1022@sohu.com)
* W Xie and M He contributed equally to this work.

migration, survival, senescence, and apoptosis [18–20]. CircRNAs are also believed to be potential diagnostic biomarkers and therapeutic targets for various diseases [21–24]. Accumulating evidence has shown that circRNA is involved in fibrogenesis and could potentially be a monitoring factor or, more excitingly, a therapeutic target for fibrosis [25–27]. To our knowledge, there are no reports on the potential role and mechanism of circRNAs in fibrogenesis of IUA so far.

In this study, we screened differential circRNA expression between IUA cell model and SIS3-treated IUA cell model. We further investigated the biological functions of selected circRNAs in the IUA cell model and attempted to elucidate the possible molecular mechanisms involved.

Materials and Methods

Ethics statement

All procedures involving animals were performed according to the guidelines of the ethical review committee of Fu Xing Hospital, Capital Medical University. Twelve female Sprague-Dawley rats, aged 10-weeks and weighing 200–250 g were housed under controlled conditions (23 ± 1.5°C, relative humidity 40–60%, 12/12 h light/dark cycle) with *ad libitum* access to food and tap water.

Isolation, purification, and culture of primary endometrial stromal cells

Endometrial stromal cells (ESCs) were isolated from rat endometrial tissues following the protocol described in a previous study [28, 29] with slight modifications. Briefly, full-thickness endometrial tissue samples were collected and kept in phosphate-buffered saline containing 100 U/ml penicillin and 100 mg/ml streptomycin (Gibco; Thermo Fisher Scientific, Waltham, MA, USA) at 4°C, and subjected to cell isolation within 30 min. The tissues were minced into < 1 mm pieces and incubated in Dulbecco's modified Eagle's medium/Nutrient Mixture F-12 (DMEM/F12; Gibco) supplemented with 200 μg/ml collagenase I (Sigma Aldrich China, Shanghai, China) for 60 min at 37°C with agitation. The dispersed endometrial tissue fragments/cells were filtered sequentially through sterile 40–100 μm nylon strainers (BD Biosciences, Shanghai, China) to remove undigested tissue clumps and epithelial cells. The dispersed cells in the second filtrate were collected by centrifugation, seeded into a collagen I-coated 25-cm tissue culture flask containing DMEM/F12 supplemented with 10% fetal bovine serum and incubated at 37°C in an atmosphere containing 5% CO_2. The medium was changed daily and the cells were monitored for confluence. The 3rd–6th passages were used for subsequent experiments.

TGF-β1-induced fibrosis and SIS3 treatment

ESCs were seeded into 6-well plates at a density of 2×10^5 cells/well for 24 h, followed by incubation with TGF-β1 (10 ng/ml, Cat. No. 80116-RNAH; Sino Biological US, Wayne, PA, USA) for 24 h to induce fibrosis (IUA model cell). These ESCs were then treated with SIS3 (3 μM, Cat. No. S7959; Selleck, Houston, TX, USA) (SIS3 group) or dimethyl sulfoxide (DMSO) (IUA group). After 48 h of treatment, the cells were harvested for reverse transcription–quantitative polymerase chain reaction (RT-qPCR) and high-throughput sequencing.

RNA extraction and quality control

Total RNA was isolated from ESCs using TRIzol reagent (Invitrogen, Carlsbad, CA, USA) following the manufacturer's instruction. Total RNA from each sample was quantified using NanoDrop ND-1000 spectrophotometer (NanoDrop, Wilmington, DE, USA). RNA integrity was assessed using Agilent 2100 Bioanalyzer Lab-on-Chip system (Agilent Technologies, Palo Alto, CA, USA) and RNA 6000 Nano LabChip Kit (Agilent Technologies). The qualified RNA fragments were used as templates for construction of circRNA-seq library using NEB Next Ultra Directional RNA Library Prep Kit (Illumina, San Diego, CA, USA) based on the manufacturer's instructions.

Screening differential circRNA expression and subsequent bioinformatics analysis

Transcriptome high-throughput sequencing and subsequent bioinformatics analysis were conducted at Guangzhou Forevergen (Guangdong, China). The prepared libraries were sequenced using Illumina Hiseq 4000 platform, and 2 × 150 bp paired-end reads (PE150) were generated according to the standard protocol of Illumina. CircRNAs were identified using DCC software [30]. EdgeR software was utilized for normalization of data and analysis of differential expression of circRNAs [31]. A circRNA–miRNA–mRNA network was constructed according to the competing endogenous RNA (ceRNA) hypothesis of circRNA [32]; a circRNA–miRNA network was constructed based on prediction of miRNA binding sites; the circRNA–miRNA–mRNA regulatory network comprised both circRNA–miRNA pairs and miRNA–mRNA pairs.

Validation of circRNAs by Sanger sequencing and qPCR

The circRNAs were validated using convergent and divergent primers designed based on the NCBI reference sequences. The details of divergent and convergent primers are listed in Table 1. The PCR products were assessed using agarose gel electrophoresis to confirm candidate circRNA junctions. Back-splicing sites of circRNAs were determined by Sanger sequencing at Tianyi Huiyuan biotechnology (Guangzhou, China).

The expression levels of candidate circRNAs were measured using quantitative real-time PCR (qPCR). qPCR was performed using SYBR Green (cat. #RR820A; TaKaRa, Dalian, China) and ABI7500 real-time PCR system (Life Technologies, Carlsbad, CA, USA) in a final volume of 20 μl. The expression of circRNAs in different ESCs was calculated using the $2^{-\Delta\Delta Ct}$ method with β-actin as the reference gene. All experiments were performed in triplicate.

Transfection of ESCs transfection with circPlekha7-targeting siRNAs and circPlekha7-overexpression plasmid

CircPlekha7-targeting siRNAs and negative controls (si-NC) were synthesized by RiboBio (Guangzhou, China). For construction of circPlekha7-overexpression plasmids, circPlekha7 cDNA was synthesized using universal primers and cloned into a pcD-ciR vector (Geenseed Biotech, Guangzhou, China), which contained a front and a back circular frame. The 3rd–6th passage ESCs were transfected with circPlekha7-targeting siRNAs, si-NC, or circPlekha7-overexpression plasmids. All cell transfections were performed using Lipofectamine 3000 (Invitrogen) following the manufacturer's protocol. The siRNAs

Table 1. Details of divergent and convergent primers

Primer ID	Primer sequences (5'-3')	Product length (bp)
R-chr16:26755422|26780008-CF1	CCTTACTTCCACGCCATGTT	216
R-chr16:26755422|26780008-CR1	AATGGGCAGTGTTTCTCAGG	
R-chr16:26755422|26780008-LF1	GAGCCGAGCAAAGAGAGTTC	104
R-chr16:26755422|26780008-LR1	CGTTTTCTTCTGTGACCTGAA	
R-chr5:158071477|158074209-CF2	CCAAGATCTTCCAGGTGGTC	163
R-chr5:158071477|158074209-CR2	TTGTGCTGCAGCTGGTTAAA	
R-chr5:158071477|158074209-LF1	GGCTATGAAGGTGGACATGG	97
R-chr5:158071477|158074209-LR1	CTTGGACACGTCTTCCGAGT	
R-chr1:185495031|185495489-CF1	AGCCAGAGGAAGACCAACCT	186
R-chr1:185495031|185495489-CR1	GGCATCTTCATAGCCTCGAC	
R-chr1:185495031|185495489-LF1	GAACGCTTCCGTTCTCAAAG	168
R-chr1:185495031|185495489-LR1	AGGTGGTAGCCCATTCCTCT	
R-chr9:52047552|52053503-CF2	GTGGCAAGGGTGATTCTGGT	183
R-chr9:52047552|52053503-CR2	CTCCTCTCTCTCCTGGCATC	
R-chr9:52047552|52053503-LF1	GGTCCTGCAGGTAACAGTGG	106
R-chr9:52047552|52053503-LR1	GAGGACCCTGAGCACCAG	
R-chr5:74954384|74956829-CF2	CCTTCCAGAACCACCTGCTA	158
R-chr5:74954384|74956829-CR2	CCCCAATTTCCATGTTTTTG	
R-chr5:74954384|74956829-LF1	AAAGAGAAAAGGGCACAGCA	190
R-chr5:74954384|74956829-LR1	TCTGCTCAGTGACGACATCC	
R-Csf1-F2	TCCTATGGGGCAAGACAAAG	195
R-Csf1-R2	TAGTGGTGGACGTTGCCATA	
rno-miR-207-F	CTTCTCCTGGCTCTCCT	57
rno-miR-207-RT	GTCGTATCCAGTGCAGGGTCCGAGGTATTCGCACTGGATACGACAAAGGG	
Universe-R	GTGCAGGGTCCGAGGT	
R-Flt1-F	TATGGCATCCCTCAGCCTAC	242
R-Flt1-R	GCCTTGCAGCTGTAGATTCC	
rno-miR-204-3p-RT	GTCGTATCCAGTGCAGGGTCCGAGGTATTCGCACTGGATACGACAACGTC	56
rno-miR-204-3p-F	GCTGGGAAGGCAAAGG	
R-α-SMA-F	ACCATCGGGAATGAACGCTT	191
R-α-SMA-R	CTGTCAGCAATGCCTGGGTA	
R-COL1(Collagen I)-F	GGAGAGAGCATGACCGATGG	184
R-COL1(Collagen I)-R	GGGACTTCTTGAGGTTGCCA	
R-Smad 3-F	CTGGGCAAGTTCTCCAGAGTT	149
R-Smad 3-R	GAAGGGCAGGATGGACGAC	

used in our study are listed in Table 2.

Cell apoptosis assay

Cell apoptosis was assessed using FITC Annexin V Apoptosis Detection Kit (BD Pharmingen, San Diego, CA, USA) 24 h post transfection following the manufacturer's instructions. The stained cells were analyzed using flow cytometry, and data were analyzed using CellQuest software (BD Bioscience).

Table 2. Details of interference fragment

Interference fragment ID	Interference fragment sequence: 5'-3'
Si-Rat-chr1185495489-1	GGATGGCAGAAGGGACAAGGT
Si-Rat-chr1185495489-2	GCAGAAGGGACAAGGTGGAAC
Si-Rat-chr1185495489-3	GGGGATGGCAGAAGGGACAA
siRNA-NC	UUCUCCGAACGUGUCACGUTT

Cell proliferation assay

Proliferation rates of ESCs were analyzed using the CellTiter 96® AQueous Non-Radioactive Cell Proliferation Assay (MTS) Kit (#G5421; Promega Biotech, Beijing, China) following the manufacturer's instructions.

Western blotting

Cells from different treatment conditions were collected and lysed in 1 × RIPA buffer (Thermo Fisher Scientific, Illinois, USA) supplemented with protease inhibitor cocktail (Roche Diagnostics GmbH, USA). The Pierce BCA protein assay kit (Thermo Fisher Scientific) was used for quantification of cellular proteins. The proteins were resolved on 12% SDS-PAGE gels and transferred to polyvinylidene fluoride (PVDF) membranes, which were blocked for 1 h in Tris-buffered saline containing 5% nonfat milk. The membranes were then incubated with primary antibodies, including those against SMAD3 (ab40854; 1:5000 dilution; Abcam, Cambridge, MA, USA), phospho-SMAD3 (Ser423/425) (C25A9) (9520, 1:1000 dilution; Cell Signaling Technology, Danvers, MA, USA), α-actin (α-SMA or 1A4, sc-32251; 1:500 dilution; Santa Cruz Biotechnology, Santa Cruz, CA, USA), collagen I (ab34710; 1:4000 dilution; Abcam), and GAPDH (Cat. No: 60004-1-Ig; 1:10000 dilution; Proteintech, Chicago, IL, USA), at 4°C overnight, followed by washing and incubation with secondary HRP-conjugated antibodies (Cat.No: SA00001-1 or Cat. No: SA00001-2; 1:4000 dilution; Sigma Aldrich, USA) for 1 h at room temperature (RT). Next, the membranes were washed thrice with tris buffered saline with tween (TBST), and protein abundances were visualized using Enhanced Chemiluminescent Reagent Kit (Boster Biological Technology, Pleasanton, CA, USA) according to the manufacturer's instructions.

Statistical analysis

All statistical analyses were performed using SPSS 19.0 software (IBM Corporation, Armonk, NY, USA). Data are expressed as mean ± standard deviation. A P-value < 0.05 was considered statistically significant.

Results

CircRNA expression profile in IUA cell model

To identify specific circRNAs that were differentially expressed between IUA and SIS3 groups, the expression profile of circRNAs was assessed through high-throughput sequencing. It was observed that the circRNA expression pattern differed between IUA and SIS3 groups. A total of 66 differentially expressed circRNAs were identified at FDR < 0.05 and log2 fold change cutoff ≥ 1, among which, 33 were upregulated and 33 were downregulated (Supplemental Table 1: online only). Scatter-plots (Fig. 1A) were generated to visualize circRNAs that were differentially expressed between IUA and SIS3 groups.

The 66 dysregulated circRNAs were distributed across almost all chromosomes (Fig. 1B). The copy number of the circRNAs was lower than 50, and the quantity was mainly below 100 (Fig. 1C); the majority of circRNAs were approximately 500 bp in length and < 200 in quantity. (Fig. 1D).

Gene Ontology (GO) and Kyoto Encyclopedia of Genes and Genomes (KEGG) pathway analyses were conducted to identify host genes of the differentially expressed circRNAs and to predict the functions of circRNAs and the molecular interactions among genes. GO enrichment analysis revealed that the most significantly enriched GO terms were associated with biological process, cellular component, and molecular function, indicating that the differentially expressed circRNAs might be closely related to binding, cellular process, and cell part. The enriched GO terms associated with biological process, cellular component, and molecular function are shown in Fig. 2A. KEGG enrichment analysis revealed the top 20 enriched pathways that involved the host genes of differentially expressed circRNAs. The host genes of the differentially expressed circRNAs were mainly enriched in the PI3K-Akt signaling pathway and protein digestion and absorption pathways (Fig. 2B).

The mRNAs of the circRNA host genes that were enriched in the PI3K-Akt signaling pathway were selected for construction and visualization of the circRNA–miRNA–mRNA network based on the ceRNA hypothesis of circRNA; the miRNAs included rno-miR-204-3p, rno-miR-455-5p, rno-miR-3578, and rno-miR-3586-3p.

The five circRNAs that intersected with the nine verified abnormally expressed circRNAs included: chr16:26755422|26780008, chr5:158071477|158074209, chr1:185495031|185495489, chr9:52047552|52053503, and chr5: 74954384|74956829. CircRNA–miRNA pairs and miRNA–mRNA pairs were combined into a circRNA–miRNA–mRNA regulatory network (Fig. 2C) comprising 24 circRNAs, 4 miRNAs, and 97 mRNAs (Supplemental Table 2: online only).

CircRNA validation and characterization of differentially expressed circRNAs

RT-qPCR was performed to assess the expression of five of the aforementioned dysregulated circRNAs in both IUA and SIS3 groups. Four among the five circRNAs (chr16:26755422|26780008, chr5:158071477|158074209, chr1:185495031|185495489, and chr5: 74954384|74956829) were expressed at higher levels in the SIS3 group than in the IUA group; one circRNA (chr9:52047552|52053503) was expressed at a lower level in SIS3 group as compared to the IUA group, consistent with the high-throughput sequencing data (Fig. 3A). The existence of selected circRNAs was validated using specific qPCR primers (Table 2). The amplified PCR products with specific circRNA junctions were then verified by Sanger sequencing using divergent primers. Nine differentially expressed circRNAs between the IUA and SIS3 groups were selected according to the following conditions: (a) circRNA with differences in expression (lower P-value and greater fold changes); and (b) circRNA host gene involved in the PI3K-Akt signaling pathway (Supplementary Table 2). The circRNAs chr16:26755422|26780008, chr5:158071477|158074209, chr1:185495031|185495489, chr9:52047552|52053503, and chr5: 74954384|74956829 were significantly amplified by PCR. These results indicate that five of the nine selected circRNAs formed a closed circular structure, suggesting the presence of back-site junctions (Fig. 3B and 3C). Chr9:52047552|52053503 from the downregulation group and chr1:185495031|185495489 from the upregulation group, with the highest fold changes, were selected for further analysis; Chr1:185495031|185495489, which overlapped with the circRNA–miRNA–mRNA regulatory network, was selected

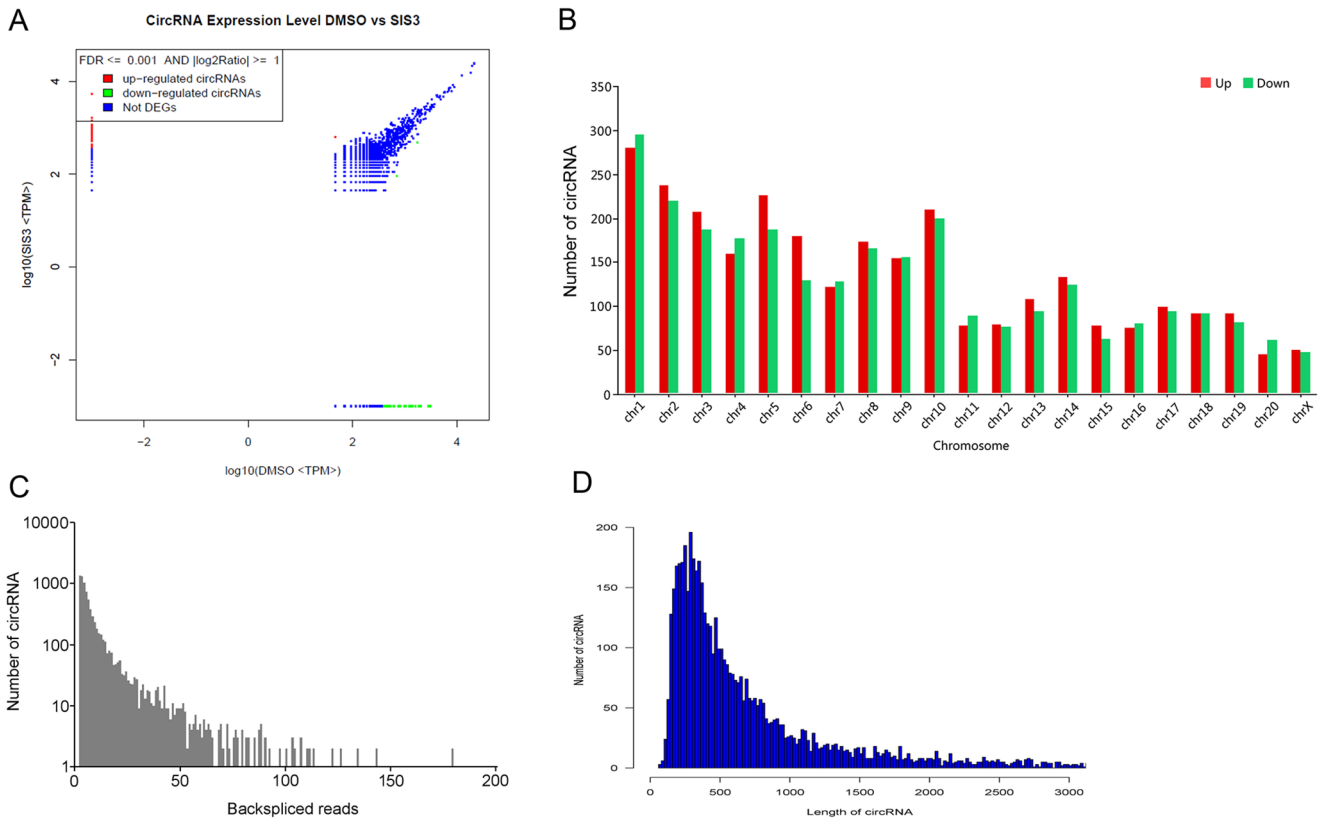

Fig. 1. Differential expression analysis of circRNAs in intrauterine adhesion (IUA) model and SIS3-treated IUA model. A: Expression level of circular RNAs (circRNAs) in IUA group *vs*. SIS3 group: blue and green, downregulation; red, upregulation. B: Chromosomal distribution of circRNAs. C: Distribution of back-spliced reads. D: Length distribution of circRNAs.

for functional investigation.

Expression of the potential target miRNAs and associated mRNAs of differentially expressed circRNAs

CircRNAs function as miRNA sponges by binding to functional miRNAs and subsequently regulate gene expression. Therefore, the potential target miRNAs and the corresponding mRNAs of two differentially expressed circRNAs were chosen based on the following criteria: predicted miRNA–mRNA binding sites ≥ 3, and mRNA involved in IUA or fibrosis. The top two circRNAs, target miRNAs, and their corresponding mRNAs, ranked by the above criteria, are shown in Supplementary Table 2. The circRNA chr1:185495031|185495489 from the upregulation group was associated with rno-miR-207 and colony-stimulating factor 1 (*Csf1*) gene, which plays a role in prevention of fibrosis [33]. The circRNA chr9:52047552|52053503 from the downregulation group was associated with rno-miR-204-3p and soluble VEGF type I receptor (*Flt1*) gene, which plays a role in fibrosis development [34]. RT-qPCR analysis demonstrated that chr1:185495031|185495489 and the related expression of *Csf1* were upregulated, whereas rno-miR-207 was downregulated in the SIS3 group as compared to the IUA group. Chr9:52047552|52053503 and the related expression of *Flt1* were downregulated, whereas rno-miR-204-3p was upregulated in the SIS3 group as compared to the IUA group (Fig. 4). These results were consistent with the ceRNA mechanism.

Detection of circPlekha7 silencing or overexpression induced by specific siRNA or circPlekha7-overexpression plasmid using qPCR

To investigate the biological functions of chr1:185495031|185495489 (circPlekha7) in the IUA group, circPlekha7 was silenced or overexpressed in ESCs using specific siRNA or circPlekha7-overexpression vector, respectively; the expression of circPlekha7 was detected using qPCR, and the results are shown in Fig. 5A. The endogenous levels of circPlekha7 were effectively reduced by 30% following transfection with three siRNAs targeting circPlekha7 as compared to transfection with si-NC; si-circPlekha7-3 significantly reduced the levels of circPlekha7 by 40% in ESCs and circPlekha7-overexpression vector significantly increased the level of circPlekha7 in ESCs. Gain- and loss-of-function assays indicated that rno-miR-207 expression was enhanced whereas *Csf1* expression was suppressed when circPlekha7 was downregulated in ESCs. However, rno-miR-207 expression was reduced and *Csf1* expression was increased when circPlekha7 was upregulated in ESCs (Fig. 5B).

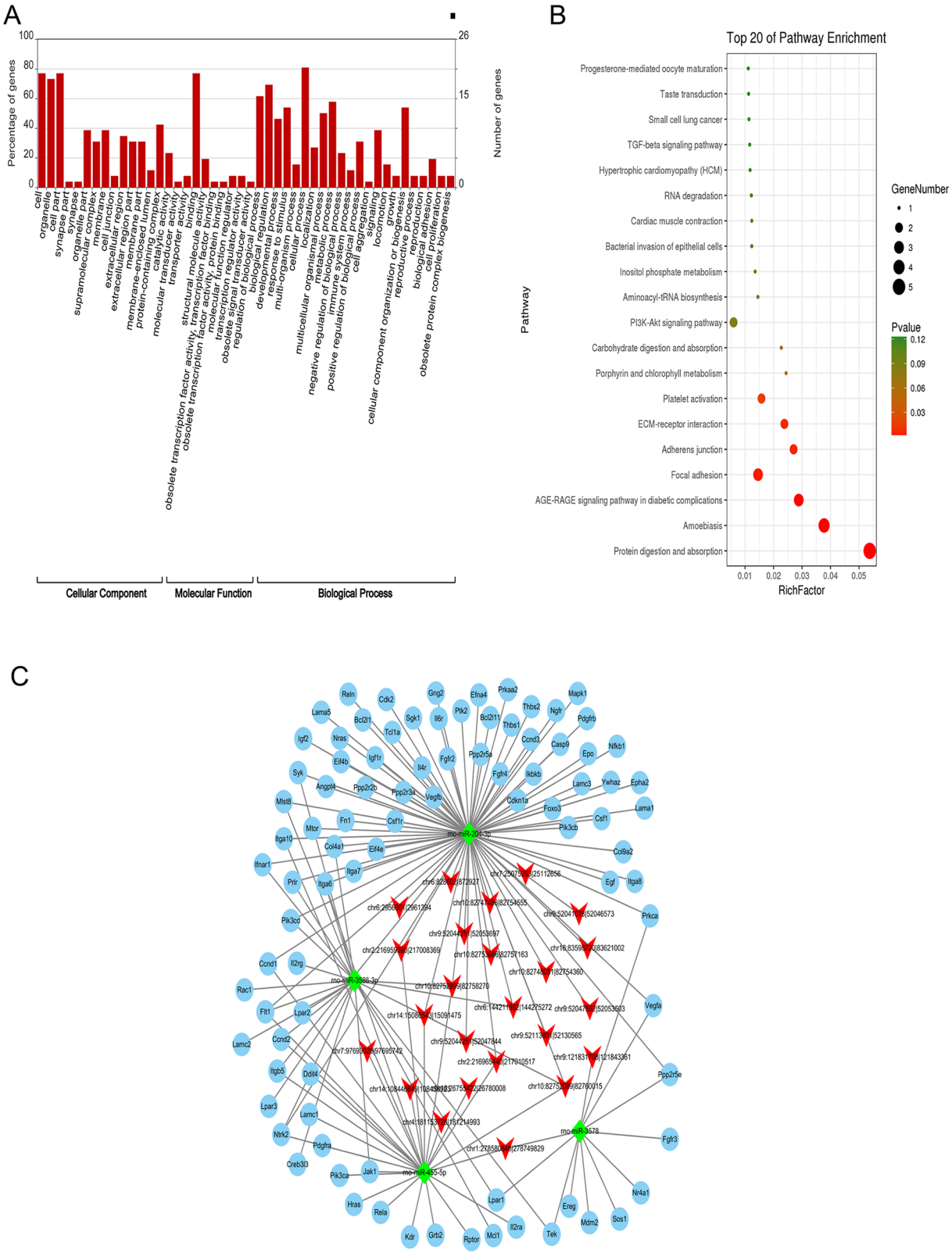

Fig. 2. Analysis of differentially expressed circular RNAs (circRNAs). A: Gene Ontology (GO) analysis of differentially expressed circRNAs. B: Kyoto Encyclopedia of Genes and Genomes (KEGG) pathway analyses of differentially expressed mRNAs. C: Predicted circRNA–miRNA–mRNA interaction networks.

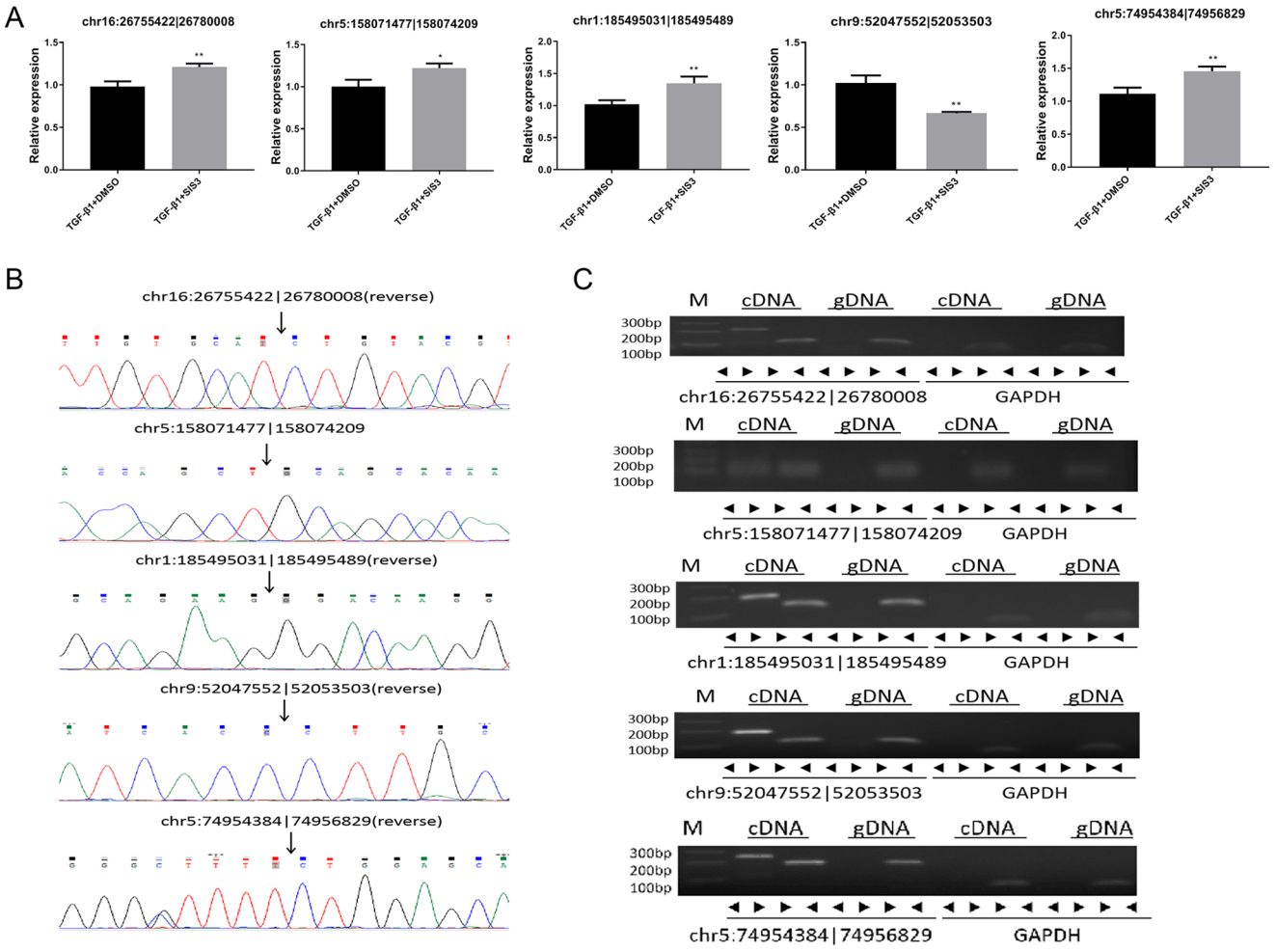

Fig. 3. Reverse transcription-quantitative polymerase chain reaction (RT-qPCR) validation of the differences in circRNA expression between neonatal and adult cattle testis. RT-qPCR data were analyzed using the $2^{-\Delta\Delta Ct}$ method, with β-*actin* as the internal control. Data are presented as mean ± s.e.m.; ** $P<0.01$, * $P<0.05$ for validation of circular RNAs (circRNAs). Electrophoretogram for circRNAs in RT-PCR. Sanger sequencing confirmed that a back-splicing junction site was present in each circRNA.

Effects of circPlekha7 on apoptosis and viability of ESCs

The effects of circPlekha7 on apoptosis of ESCs were assessed using flow cytometry. In the IUA group, CircPlekha7 knockdown remarkably reduced cell apoptosis, while circPlekha7 overexpression increased the proportion of apoptotic cells as compared to control (Fig. 6A). SIS3 treatment promoted apoptosis of circPlekha7-overexpressed ESCs but had little effect on circPlekha7-silenced ESCs (Fig. 6B). MTS demonstrated that knockdown of circPlekha7 increased cell viability, whereas overexpression of circPlekha7 decreased cell viability at 72 h post transfection as compared to the control group. SIS3 treatment further inhibited the viability of circPlekha7-overexpressed ESCs but had little effect on circPlekha7-silenced ESCs (Fig. 6C and 6D). These results indicate that circPlekha7 promotes apoptosis and reduces the viability of ESCs, and SIS3 further enhances these effects in circPlekha7-overexpressed ESCs.

Effects of circPlekha7 on fibrosis-related proteins

The effects of circPlekha7 on fibrosis-related proteins and their mRNA levels were demonstrated using western blotting and RT-qPCR. Overexpression of circPlekha7 suppressed the levels of α-SMA, collagen I, SMAD3, and pSMAD3 proteins; whereas knockdown of circPlekha7 enhanced the levels of these proteins in IUA cell model (Fig. 7A). SIS3 treatment further downregulated the expression of the aforementioned fibrosis-related proteins in circPlekha7-overexpressed ESCs but not in circPlekha7-silenced ESCs (Fig. 7B). Similarly, overexpression of circPlekha7 suppressed mRNA expression levels of *α-SMA*, *collagen I*, and *Smad3*; whereas knockdown of circPlekha7 enhanced the mRNA expression levels of these genes in IUA cell model (Fig. 7C). SIS3 treatment further reduced the mRNA expression levels of the aforementioned genes in circPlekha7-overexpressed ESCs but not in circPlekha7-silenced ESCs (Fig. 7D). We also showed that SIS3 treatment significantly inhibited SMAD3 phosphorylation as well as *α-SMA* and *Collagen*

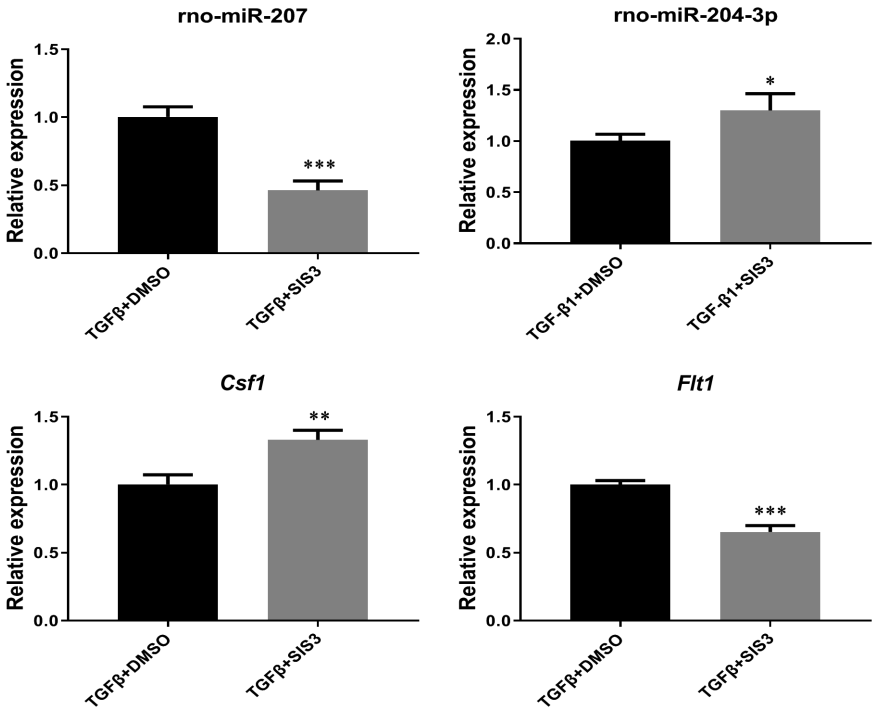

Fig. 4. Expression of miRNAs and mRNAs associated with the differentially expressed circular RNAs (circRNAs). * P < 0.05; ** P < 0.01; *** P < 0.001.

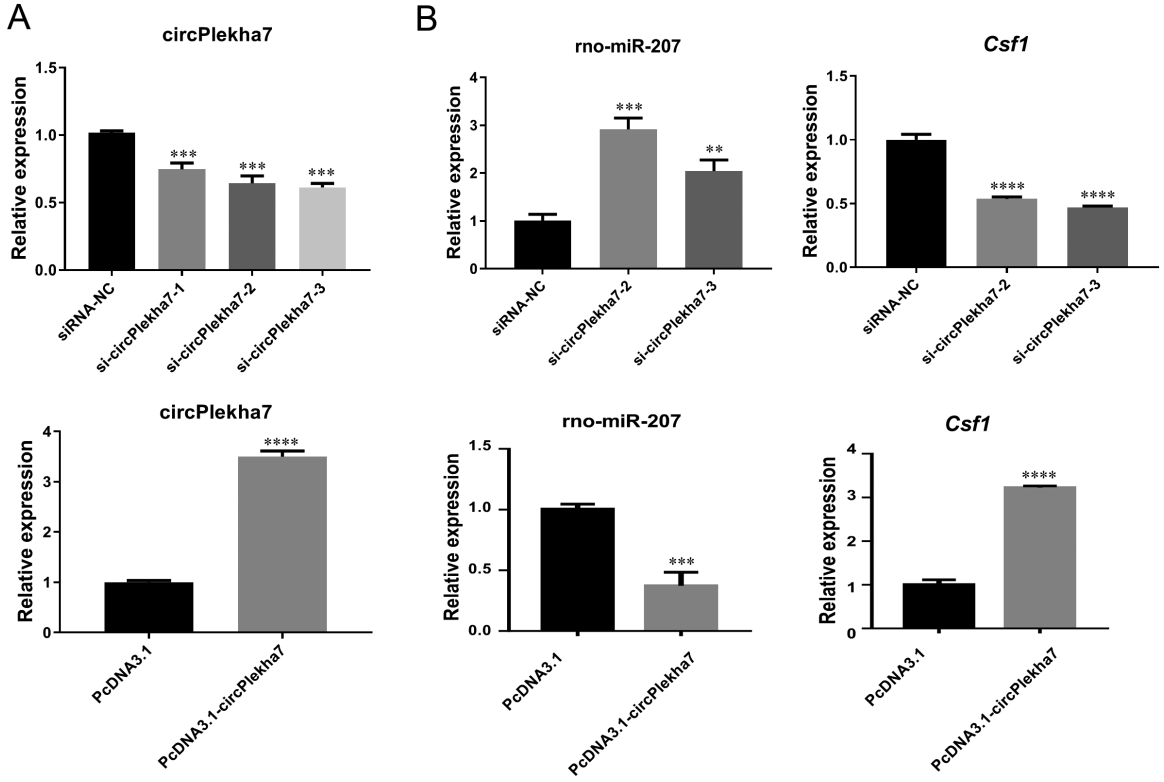

Fig. 5. A: Efficacy of circPlekha7-targeting siRNA and circPlekha7-overexpression vector detected using reverse transcription-quantitative polymerase chain reaction (RT-qPCR). B: Expression of miRNAs and mRNAs after circPlekha7 knockdown and overexpression. ** P < 0.01; *** P < 0.001; **** P < 0.0001.

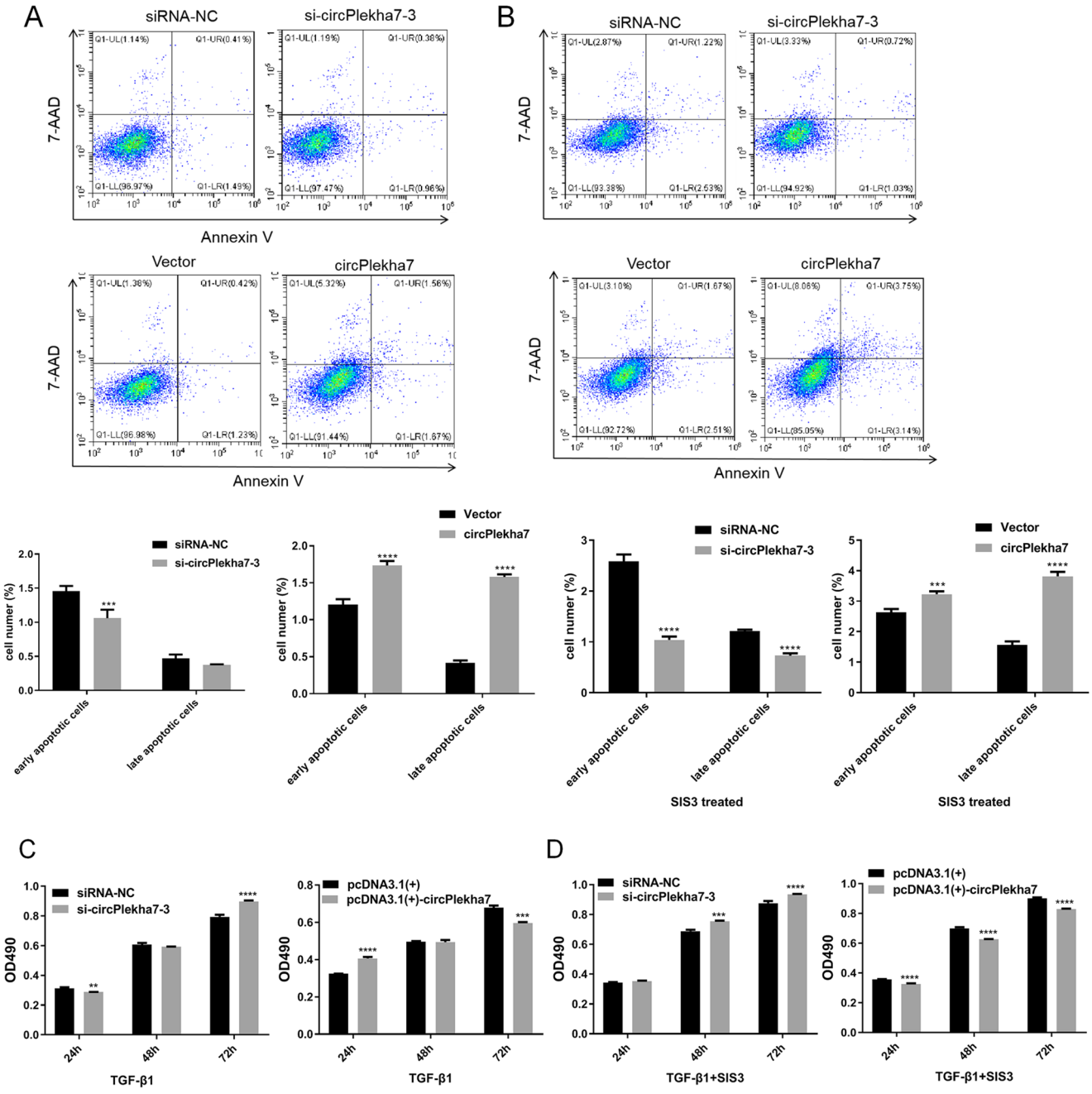

Fig. 6. Alterations in fibrosis-induced endometrial stromal cells (ESCs) after circPlekha7 knockdown or overexpression. A: Analysis of apoptosis in fibrosis-induced ESCs after circPlekha7 knockdown or overexpression. B: Analysis of apoptosis in SIS3-treated fibrosis induced-ESCs after circPlekha7 knockdown or overexpression C: Proliferation of fibrosis induced-ESCs at different time-points after circPlekha7 knockdown or overexpression detected using MTS. D: Proliferation of SIS3-treated fibrosis induced-ESCs at different time points after circPlekha7 knockdown or overexpression detected using MTS. ** $P < 0.01$; *** $P < 0.001$; **** $P < 0.0001$.

I expression (Supplemental Fig. 1: online only). The above results indicate that circPlekha7 inhibits the expression of fibrosis-related proteins, and the SMAD3 inhibitor SIS3 inhibits fibrosis by targeting circPlekha7.

Discussion

IUA is a common gynecological disease caused by damage to the endometrial basement membrane and exposure of myometrial tissue [5]. It is characterized by the destruction of the border between the

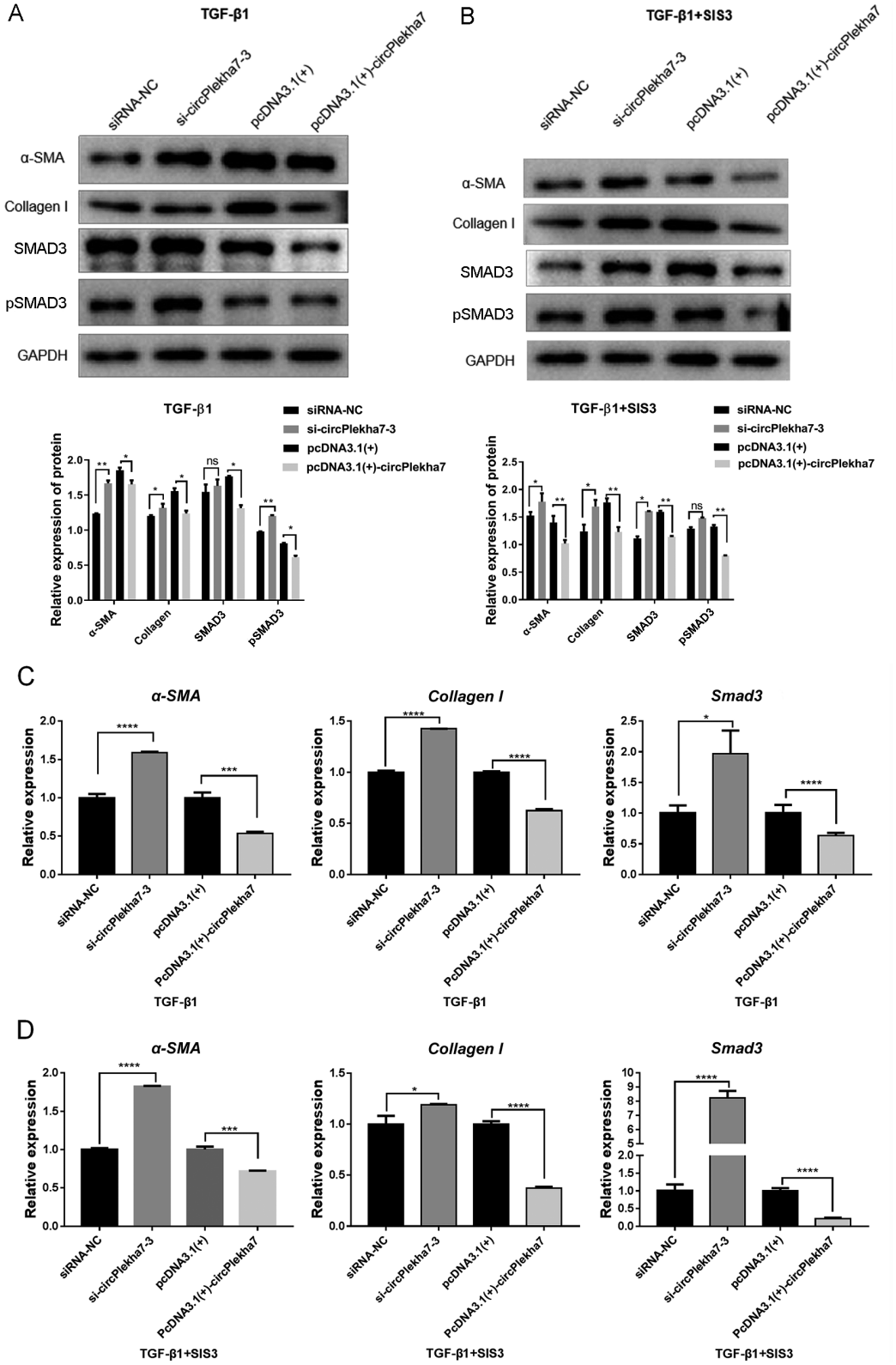

Fig. 7. Effects of circPlekha7 on the protein and mRNA expression levels of fibrosis-related proteins. A and B: Levels of α-SMA, collagen I, SMAD3, and pSMAD3 proteins in circPlekha-silenced and circPlekha-overexpressed ESCs determined using western blotting. C and D: mRNA expression levels of *α-SMA, collagen I*, *and Smad3* in circPlekha-silenced and circPlekha-overexpressed endometrial stromal cells (ESCs) determined using reverse transcription-quantitative polymerase chain reaction (RT-qPCR). * $P < 0.05$; ** $P < 0.01$; *** $P < 0.001$; **** $P < 0.0001$.

basal and functional endometrial layers due to endometrial trauma or uterine infections [35].

In this study, we established an IUA cell model by treating ESCs isolated from rat uterus with TGF-β1, and used SIS3 to reverse TGF-β1-induced fibrosis in ESCs. We screened out 66 differentially expressed circRNAs between the IUA and SIS3 groups. Among these, circPlekha7 was significantly upregulated in the SIS3 group. Overexpression of circPlekha7 enhanced apoptosis, decreased the viability of ESCs, and suppressed the expression of *α-SMA*, *collagen I*, and *SMAD3* in ESCs. SIS3 treatment enhanced these effects in circPlekha7-overexpressed ESCs but not in circPlekha7-silenced ESCs. The results indicate that circPlekha7 plays an anti-fibrotic role in IUA cell model, and SIS3 inhibits fibrosis by targeting circPlekha7.

Although the function of circPlekha7 has not been reported yet, the function of the parent gene *PLEKHA7* has been recognized. It is reported that *PLEKHA7* induces changes in the asset of E-cadherin-containing cell-cell contacts, thus inhibiting E-cadherin/EGFR crosstalk and leading to a less aggressive tumor phenotype [36]. *PLEKHA7* regulates the levels of certain miRNAs, particularly miR-30b, to suppress the expression of cell transformation markers [37]. *PLEKHA7* also plays a role in E-cadherin-mediated tumor progression by binding to cadherin complexes [38]. However, the role of *PLEKHA* in IUA has not been studied yet, and our study is the first to reveal the anti-fibrotic role of circPlekha7 in IUA.

Emerging evidence has shown that circRNA is involved in fibrosis and is a potential diagnostic biomarker and therapeutic target for fibrosis. The host genes of the differentially expressed circRNAs were involved in the regulation of cell cycle, adherens junctions, and RNA transport [25]. The mechanism of fibrosis involves multiple signaling pathways, including the PI3K/Akt/mTOR, AMPK, and TGF-β/VEGF pathways. Specifically, PI3K/Akt/mTOR pathway plays a crucial role in the development of fibrosis via regulation of several upstream and downstream factors [39]. We found that the host genes of the differentially expressed circRNAs in the IUA cell model were mainly enriched in the PI3K-Akt signaling pathway. Therefore, the mRNAs of the circRNA host genes participating in the PI3K-Akt signaling pathway were selected for construction and visualization of the circRNA–miRNA–mRNA network; several parental genes of the differentially expressed circRNAs were found to be associated with the biological process of fibrosis. The role of circRNAs in fibrosis, including pulmonary fibrosis [25], cardiac fibrosis [26], liver fibrosis [40], and keloid scaring [41], has been gradually recognized and confirmed. CircRNAs mainly function as miRNA sponges; therefore, circRNAs are believed to negatively regulate miRNAs, contributing substantially to the ceRNA network [42]. The circRNA/miRNA interaction analysis indicated that abnormally expressed circRNAs in the IUA cell model possessed miRNA target sites that play important roles in fibrosis. Targeted miRNAs of the differentially expressed circRNAs, rno-miR-204-3p and rno-miR-207, reportedly participate in cell proliferation, apoptosis, migration, epithelial–mesenchymal transition (EMT), and cytoskeleton remodeling [43]. Further, the role and downstream targets of rno-miR-204-3p and rno-miR-207 in the IUA cell model were investigated. It was observed that two genes, *Flt1* and *Csf1*, associated with the differentially expressed circRNAs played important roles in protection against fibrosis.

Additionally, we found that circPlekha7 was specifically overexpressed in normal reversed ESCs. Functional knockdown and overexpression experiments confirmed that circPlekha7 plays an important role in cell apoptosis and EMT. The characteristic feature of EMT is the replacement of epithelial cell adhesion molecules, including E-cadherin and zonula occludens-1 (ZO-1), with mesenchymal markers, including α-SMA, collagens, vimentin, and matrix metalloproteinase (MMP)-2, and MMP-9 [44, 45]. Our study also suggests that SIS3 acts as a SMAD3 inhibitor and inhibits fibrosis by targeting circPlekha7. SMAD3 is a key element of the signal transduction pathways involved in fibrosis development [46]. A number of fibrogenic genes (collagen) and markers (α-SMA and E-cadherin) are SMAD3-dependent, and SMAD3 regulates these genes by directly binding to the corresponding DNA sequences [47, 48]. Thus, circPlekha7 may act as a target of SMAD3 in order to exert its anti-fibrotic effects; .

In conclusion, the present study demonstrates that dysregulated circRNAs may be involved in pro- or anti-fibrotic signaling pathways in IUA by targeting miRNAs or by regulating their host genes. Overexpression of circPlekha7 enhanced apoptosis, decreased the viability of ESCs, and suppressed the expression of *α-SMA*, *collagen I*, and *SMAD3* in ESCs, whereas knockdown of circPlekha7 exhibited opposite results. Moreover, circPlekha7 acts as a target of the SMAD3 inhibitor SIS3 to exert its anti-fibrotic effects. Our study provides valuable information for improving the understanding of the regulatory mechanisms involved in IUA and provides a base for the development of novel approaches for diagnosis, treatment, and prevention of IUA.

Conflict of interest: The authors declare no conflicts of interest.

Acknowledgement

This work was supported by the National Natural Science Foundation of China.

References

1. **Asherman JG.** Amenorrhoea traumatica (atretica). *J Obstet Gynaecol Br Emp* 1948; **55**: 23–30. [Medline] [CrossRef]
2. **Asherman J.** Traumatic intrauterine adhesions and their effects on fertility. *Int J Fertil* 1957; **2**: 49–61.
3. **Asherman JG.** Traumatic intra-uterine adhesions. *J Obstet Gynaecol Br Emp* 1950; **57**: 892–896. [Medline] [CrossRef]
4. **Santamaria X, Isaacson K, Simón C.** Asherman's syndrome: it may not be all our fault. *Hum Reprod* 2018; **33**: 1374–1380. [Medline] [CrossRef]
5. **Yu D, Wong Y-M, Cheong Y, Xia E, Li T-C.** Asherman syndrome—one century later. *Fertil Steril* 2008; **89**: 759–779. [Medline] [CrossRef]
6. **Leask A, Abraham DJ.** TGF-β signaling and the fibrotic response. *FASEB J* 2004; **18**: 816–827. [Medline] [CrossRef]
7. **Overall CM, Wrana JL, Sodek J.** Independent regulation of collagenase, 72-kDa progelatinase, and metalloendoproteinase inhibitor expression in human fibroblasts by transforming growth factor-beta. *J Biol Chem* 1989; **264**: 1860–1869. [Medline]
8. **Branton MH, Kopp JB.** TGF-β and fibrosis. *Microbes Infect* 1999; **1**: 1349–1365. [Medline] [CrossRef]
9. **Mead AL, Wong TT, Cordeiro MF, Anderson IK, Khaw PT.** Evaluation of anti-TGF-β2 antibody as a new postoperative anti-scarring agent in glaucoma surgery. *Invest Ophthalmol Vis Sci* 2003; **44**: 3394–3401. [Medline] [CrossRef]
10. **Miettinen PJ, Ebner R, Lopez AR, Derynck R.** TGF-beta induced transdifferentiation of mammary epithelial cells to mesenchymal cells: involvement of type I receptors. *J Cell Biol* 1994; **127**: 2021–2036. [Medline] [CrossRef]
11. **Scharenberg MA, Pippenger BE, Sack R, Zingg D, Ferralli J, Schenk S, Martin I,**

Chiquet-Ehrismann R. TGF-β-induced differentiation into myofibroblasts involves specific regulation of two MKL1 isoforms. *J Cell Sci* 2014; **127**: 1079–1091. [Medline] [CrossRef]
12. **Lan HY, Chung AC.** Transforming growth factor-β and Smads. Diabetes and the Kidney: Karger Publishers, 2011: 75–82.
13. **Jinnin M, Ihn H, Tamaki K.** Characterization of SIS3, a novel specific inhibitor of Smad3, and its effect on transforming growth factor-β1-induced extracellular matrix expression. *Mol Pharmacol* 2006; **69**: 597–607. [Medline] [CrossRef]
14. **Li J, Qu X, Yao J, Caruana G, Ricardo SD, Yamamoto Y, Yamamoto H, Bertram JF.** Blockade of endothelial-mesenchymal transition by a Smad3 inhibitor delays the early development of streptozotocin-induced diabetic nephropathy. *Diabetes* 2010; **59**: 2612–2624. [Medline] [CrossRef]
15. **Memczak S, Jens M, Elefsinioti A, Torti F, Krueger J, Rybak A, Maier L, Mackowiak SD, Gregersen LH, Munschauer M, Loewer A, Ziebold U, Landthaler M, Kocks C, le Noble F, Rajewsky N.** Circular RNAs are a large class of animal RNAs with regulatory potency. *Nature* 2013; **495**: 333–338. [Medline] [CrossRef]
16. **Sanger HL, Klotz G, Riesner D, Gross HJ, Kleinschmidt AK.** Viroids are single-stranded covalently closed circular RNA molecules existing as highly base-paired rod-like structures. *Proc Natl Acad Sci USA* 1976; **73**: 3852–3856. [Medline] [CrossRef]
17. **Cheng Y, Sun H, Wang H, Jiang W, Tang W, Lu C, Zhang W, Chen Z, Lv C.** Star circular RNAs in human cancer: progress and perspectives. *Onco Targets Ther* 2019; **12**: 8249–8261. [Medline] [CrossRef]
18. **Vo JN, Cieslik M, Zhang Y, Shukla S, Xiao L, Zhang Y, Wu Y-M, Dhanasekaran SM, Engelke CG, Cao X, Robinson DR, Nesvizhskii AI, Chinnaiyan AM.** The landscape of circular RNA in cancer. *Cell* 2019; **176**: 869–881.e13. [Medline] [CrossRef]
19. **Shang B-Q, Li M-L, Quan HY, Hou P-F, Li Z-W, Chu S-F, Zheng J-N, Bai J.** Functional roles of circular RNAs during epithelial-to-mesenchymal transition. *Mol Cancer* 2019; **18**: 138. [Medline] [CrossRef]
20. **Yu C-Y, Kuo H-C.** The emerging roles and functions of circular RNAs and their generation. *J Biomed Sci* 2019; **26**: 29. [Medline] [CrossRef]
21. **Wang W, Wang Y, Piao H, Li B, Huang M, Zhu Z, Li D, Wang T, Xu R, Liu K.** Circular RNAs as potential biomarkers and therapeutics for cardiovascular disease. *PeerJ* 2019; **7**: e6831. [Medline] [CrossRef]
22. **Lei B, Tian Z, Fan W, Ni B.** Circular RNA: a novel biomarker and therapeutic target for human cancers. *Int J Med Sci* 2019; **16**: 292–301. [Medline] [CrossRef]
23. **Zhang Z, Yang T, Xiao J.** Circular RNAs: promising biomarkers for human diseases. *EBioMedicine* 2018; **34**: 267–274. [Medline] [CrossRef]
24. **Yao G, Niu W, Zhu X, He M, Kong L, Chen S, Zhang L, Cheng Z.** *hsa_circRNA_104597*: a novel potential diagnostic and therapeutic biomarker for schizophrenia. *Biomarkers Med* 2019; **13**: 331–340. [Medline] [CrossRef]
25. **Li R, Wang Y, Song X, Sun W, Zhang J, Liu Y, Li H, Meng C, Zhang J, Zheng Q, Lv C.** Potential regulatory role of circular RNA in idiopathic pulmonary fibrosis. *Int J Mol Med* 2018; **42**: 3256–3268. [Medline]
26. **Zhu Y, Pan W, Yang T, Meng X, Jiang Z, Tao L, Wang L.** Upregulation of circular RNA circNFIB attenuates cardiac fibrosis by sponging miR-433. *Front Genet* 2019; **10**: 564. [Medline] [CrossRef]
27. **Yang L, Yang F, Zhao H, Wang M, Zhang Y.** Circular RNA circCHFR facilitates the proliferation and migration of vascular smooth muscle via miR-370/FOXO1/Cyclin D1 pathway. *Mol Ther Nucleic Acids* 2019; **16**: 434–441. [Medline] [CrossRef]
28. **Masuda A, Katoh N, Nakabayashi K, Kato K, Sonoda K, Kitade M, Takeda S, Hata K, Tomikawa J.** An improved method for isolation of epithelial and stromal cells from the human endometrium. *J Reprod Dev* 2016; **62**: 213–218. [Medline] [CrossRef]
29. **Ryan IP, Schriock ED, Taylor RN.** Isolation, characterization, and comparison of human endometrial and endometriosis cells in vitro. *J Clin Endocrinol Metab* 1994; **78**: 642–649. [Medline]
30. **Cheng J, Metge F, Dieterich C.** Specific identification and quantification of circular RNAs from sequencing data. *Bioinformatics* 2016; **32**: 1094–1096. [Medline] [CrossRef]
31. **Lun AT, Chen Y, Smyth GK.** It's DE-licious: a recipe for differential expression analyses of RNA-seq experiments using quasi-likelihood methods in edgeR. Statistical Genomics: Springer, 2016: 391–416.
32. **Salmena L, Poliseno L, Tay Y, Kats L, Pandolfi PP.** A ceRNA hypothesis: the Rosetta Stone of a hidden RNA language? *Cell* 2011; **146**: 353–358. [Medline] [CrossRef]
33. **Menke J, Iwata Y, Rabacal WA, Basu R, Yeung YG, Humphreys BD, Wada T, Schwarting A, Stanley ER, Kelley VR.** CSF-1 signals directly to renal tubular epithelial cells to mediate repair in mice. *J Clin Invest* 2009; **119**: 2330–2342. [Medline] [CrossRef]
34. **Motomura Y, Kanbayashi H, Khan WI, Deng Y, Blennerhassett PA, Margetts PJ, Gauldie J, Egashira K, Collins SM.** The gene transfer of soluble VEGF type I receptor (Flt-1) attenuates peritoneal fibrosis formation in mice but not soluble TGF-β type II receptor gene transfer. *Am J Physiol Gastrointest Liver Physiol* 2005; **288**: G143–G150. [Medline] [CrossRef]
35. **Healy MW, Schexnayder B, Connell MT, Terry N, DeCherney AH, Csokmay JM, Yauger BJ, Hill MJ.** Intrauterine adhesion prevention after hysteroscopy: a systematic review and meta-analysis. *Am J Obstet Gynecol* 2016; **215**: 267–275.e7. [Medline] [CrossRef]
36. **Rea K, Roggiani F, De Cecco L, Raspagliesi F, Carcangiu ML, Nair-Menon J, Bagnoli M, Bortolomai I, Mezzanzanica D, Canevari S, Kourtidis A, Anastasiadis PZ, Tomassetti A.** Simultaneous E-cadherin and PLEKHA7 expression negatively affects E-cadherin/EGFR mediated ovarian cancer cell growth. *J Exp Clin Cancer Res* 2018; **37**: 146. [Medline] [CrossRef]
37. **Kourtidis A, Ngok SP, Pulimeno P, Feathers RW, Carpio LR, Baker TR, Carr JM, Yan IK, Borges S, Perez EA, Storz P, Copland JA, Patel T, Thompson EA, Citi S, Anastasiadis PZ.** Distinct E-cadherin-based complexes regulate cell behaviour through miRNA processing or Src and p120 catenin activity. *Nat Cell Biol* 2015; **17**: 1145–1157. [Medline] [CrossRef]
38. **Kourtidis A, Lu R, Pence LJ, Anastasiadis PZ.** A central role for cadherin signaling in cancer. *Exp Cell Res* 2017; **358**: 78–85. [Medline] [CrossRef]
39. **Dou F, Liu Y, Liu L, Wang J, Sun T, Mu F, Guo Q, Guo C, Jia N, Liu W, Ding Y, Wen A.** Aloe-emodin ameliorates renal fibrosis via inhibiting PI3K/Akt/mTOR signaling pathway in vivo and in vitro. *Rejuvenation Res* 2019; **22**: 218–229. [Medline] [CrossRef]
40. **Zhou Y, Lv X, Qu H, Zhao K, Fu L, Zhu L, Ye G, Guo J.** Differential expression of circular RNAs in hepatic tissue in a model of liver fibrosis and functional analysis of their target genes. *Hepatol Res* 2019; **49**: 324–334. [Medline] [CrossRef]
41. **Shi J, Yao S, Chen P, Yang Y, Qian M, Han Y, Wang N, Zhao Y, He Y, Lyu L.** The integrative regulatory network of circRNA and microRNA in keloid scarring. *Mol Biol Rep* 2020; **47**: 201–209. [Medline]
42. **Kulcheski FR, Christoff AP, Margis R.** Circular RNAs are miRNA sponges and can be used as a new class of biomarker. *J Biotechnol* 2016; **238**: 42–51. [Medline] [CrossRef]
43. **Wang Y, Li W, Zang X, Chen N, Liu T, Tsonis PA, Huang Y.** MicroRNA-204-5p regulates epithelial-to-mesenchymal transition during human posterior capsule opacification by targeting SMAD4. *Invest Ophthalmol Vis Sci* 2013; **54**: 323–332. [Medline] [CrossRef]
44. **Bi WR, Xu GT, Lv LX, Yang CQ.** The ratio of transforming growth factor-β1/bone morphogenetic protein-7 in the progression of the epithelial-mesenchymal transition contributes to rat liver fibrosis. *Genet Mol Res* 2014; **13**: 1005–1014. [Medline] [CrossRef]
45. **Zhang Y, Wei J, Wang H, Xue X, An Y, Tang D, Yuan Z, Wang F, Wu J, Zhang J, Miao Y.** Epithelial mesenchymal transition correlates with CD24+CD44+ and CD133+ cells in pancreatic cancer. *Oncol Rep* 2012; **27**: 1599–1605. [Medline]
46. **Medeiros AI, Sá-Nunes A, Soares EG, Peres CM, Silva CL, Faccioli LH.** Blockade of endogenous leukotrienes exacerbates pulmonary histoplasmosis. *Infect Immun* 2004; **72**: 1637–1644. [Medline] [CrossRef]
47. **Latella G, Vetuschi A, Sferra R, Catitti V, D'Angelo A, Zanninelli G, Flanders KC, Gaudio E.** Targeted disruption of Smad3 confers resistance to the development of dimethylnitrosamine-induced hepatic fibrosis in mice. *Liver Int* 2009; **29**: 997–1009. [Medline] [CrossRef]
48. **Masszi A, Kapus A.** Smaddening complexity: the role of Smad3 in epithelial-myofibroblast transition. *Cells Tissues Organs* 2011; **193**: 41–52. [Medline] [CrossRef]